Journal of
*Composites Science*

MDPI

*Article*

# The Antioxidant Protective Effect of Iris-Squid-Derived Protein Hydrolysates (>10 kDa) in HSF Fibroblast Cells Induced by $H_2O_2$

**Na Li [1], Xiaozhen Diao [1], Xinyi Pu [1], Pengjie Tang [1], Jeevithan Elango [1,2,3,*] and Wenhui Wu [1,4,5,*]**

[1] Department of Marine Pharmacology, College of Food Science and Technology, Shanghai Ocean University, Shanghai 201306, China; 18335440803@163.com (N.L.); xzdiao@shou.edu.cn (X.D.); pxy990129@163.com (X.P.); 15722869010@163.com (P.T.)
[2] Department of Biomaterials Engineering, Faculty of Health Sciences, UCAM-Universidad Católica San Antonio de Murcia, Guadalupe, 30107 Murcia, Spain
[3] Center of Molecular Medicine and Diagnostics (COMManD), Department of Biochemistry, Saveetha Dental College and Hospitals, Saveetha Institute of Medical and Technical Sciences, Saveetha University, Chennai 600077, India
[4] Marine Biomedical Science and Technology Innovation Platform of Lin-Gang Special Area, Shanghai 201306, China
[5] Putuo Branch of International Combined Research Center for Marine Biological Sciences, Zhoushan 316104, China
* Correspondence: srijeevithan@gmail.com or jelango@ucam.edu (J.E.); whwu@shou.edu.cn (W.W.)

**Abstract:** One of the supporting factors behind the biomolecules recently used in anti-aging and skin nourishment is their antioxidant properties. Hydrogen peroxide ($H_2O_2$) is a well-known small molecule oxidant that induces apoptosis in human skin fibroblast (HSF) cells through the synthesis of inflammatory cytokines. Hence, this study aimed to investigate the antioxidant activities of protein hydrolysates prepared from Iris squid (*Symplectoteuthis oualaniensis*) (PHCSO) in vitro. Firstly, two peptides with MWs more than 10 kDa (PHCSO-1) and less than 10 kDa (PHCSO-2) were obtained through ultrafiltration and were characterized (molecular pattern amino acid composition, FTIR) before testing the antioxidant activity (DPPH radical scavenging activity and hydroxyl radical scavenging activity). Then, the effects of PHCSOs on HSF cell viability, $H_2O_2$-induced oxidative stress model of HSF cells, ROS fluorescence staining, level of cytokines (IL-1, IL-6 and TNF-α) and cellular antioxidant properties (SOD activity, CAT activity, GSH and MDA content) were investigated. The cell morphology was examined through fluorescence staining and inflammatory factors and antioxidant activity analysis showed that superior properties were observed in PHCSO-2 peptide compared to PHCSO-1 and PHCSO. Among the peptides, PHCSO-2 (5 mg/mL) had higher DPPH and hydroxyl radical scavenging activities of 58% and 57%, respectively. On the other hand, the PHCSO-2 treatment reduced the TNF-α activity by 25%, which indicated the effective protection of PHCSO-2 from oxidative stress damage in the skin. These findings proved that peptides with less than 10 kDa were more suitable for therapeutic purposes, with good antioxidant properties. Accordingly, the protein hydrolysate from *S. oualaniensis* proved to be an excellent marine-based antioxidant peptide, which could be applied in cosmetic, pharmaceutical and food industries.

**Keywords:** hydrolysate; $H_2O_2$ oxidative stress; antioxidant activity; inflammatory cytokines; fibroblast



**Citation:** Li, N.; Diao, X.; Pu, X.; Tang, P.; Elango, J.; Wu, W. The Antioxidant Protective Effect of Iris-Squid-Derived Protein Hydrolysates (>10 kDa) in HSF Fibroblast Cells Induced by $H_2O_2$. *J. Compos. Sci.* **2023**, *7*, 228. https://doi.org/10.3390/jcs7060228

Academic Editor: Francesco Tornabene

Received: 14 April 2023
Revised: 16 May 2023
Accepted: 1 June 2023
Published: 3 June 2023



## 1. Introduction

Natural products extracted from marine organisms are beneficial to human health due to their specific living environment, which has been attracting continuous attention. Proteins with antioxidant activity produced by marine organisms have been undergoing screening for potential antioxidants for years to be further applied in cosmetic, pharmaceutical and food industries. [1] Free radicals are the core factors of skin aging [2,3]. While

inducing HSF cells apoptosis through the biofilm system, hydrogen peroxide ($H_2O_2$) is decomposed to produce OH free radicals that can trigger the degradation of hyaluronic acid, probably with the continuous generation of new $H_2O_2$ [4,5]. In addition, oxidative stress induced by $H_2O_2$ leads to the synthesis of inflammatory cytokines such as IL-1, IL-6 and TNF-α, which are involved in the regulation of skin inflammation and irritation. The biological activity of protein peptides has been extensively studied since it was first introduced by Marcuse [6]. Antioxidant peptides commonly contain 5–16 amino acid residues [7].

*S. oualaniensis* is one kind of deep-sea animal that inhabits a dark environment characterized by high pressure, low temperature and low oxygen. It shows fine growth characteristics with a short growth cycle and fast reproduction rate, contributing to its great potential in the production of new bioactive compounds, which could be a resource of marine protein that is worthwhile for exploitation [8]. China owns rich Iris squid resources that have high protein content, which are mainly distributed in the Indian Ocean and the South China Sea [9]. Much evidence has been provided concerning the good biological activity of Iris squid. Protease hydrolysates isolated from *S. oualaniensis* can be used to develop natural antioxidants and functional foods, which could show promising effects on health [10,11].

As the largest body part of the *S. oualaniensis*, the carcass contains high protein and low fat (17.24% and 0.49% of fresh weight, respectively) [12], which can be a high-quality protein source. The proteins extracted from the carcass of squid were hydrolyzed using protease at a specific cleavage site to produce small molecular peptides and free amino acids, which were easily absorbed with high activity [13]. It has been confirmed that the proteins have certain antioxidant activity [14,15], hypoglycemic activity [16] and other biological activities, which have wide applications in the cosmetic and pharmaceutical industries. However, most of the previous studies focused on the protein extracted from Iris squid instead of the antioxidant peptides from the carcasses, which remain to be explored. Therefore, in this study, protein protease hydrolysates from the carcass of Iris squid (*S. oualaniensis*) were prepared to be investigated for their antioxidant activities in vitro, providing a theoretical basis for further application in the industry.

## 2. Materials and Methods

### 2.1. Materials

Citric acid (CA), sodium hydroxide (NaOH), hydrochloric acid (HCl), concentrated sulfuric acid ($H_2SO_4$), potassium sulphate ($K_2SO_4$), cupric sulfate ($CuSO_4$) and hydrogen peroxide ($H_2O_2$) were purchased from Sinopharm Chemical Reagent Co., Ltd. (Shanghai, China). 1,1-diphenyl-2-picrylhydrazyl radical 2 was purchased from Tokyo Chemical Industry (Shanghai, China). 2,7-dichlorodihydrofluorescein diacetate was purchased from Sigma-Aldrich (St. Louis, MI, USA). Pepsin and trypsin were purchased from Shanghai McLean Biochemical Technology Co., Ltd. (Shanghai, China). The SDS-PAGE gel preparation kit was purchased from Beijing Solaibao Technology Co., Ltd. (Beijing, China). HSF cells and fetal bovine serum (FBS) were purchased from Grand Biological Co.Ltd, (Gibco BRL, Grand Island, NY, USA). All of the reagents were used at analytical grade unless otherwise specified.

### 2.2. Preparation of Carcass Protein from S. oualaniensis

Iris squids (*S. oualaniensis*) were fished in the northwest part of the Indian Ocean by the Fisheries College of Shanghai Ocean University. The squids were thawed at room temperature at about 27 °C and washed thoroughly with tap water, and then the head and foot were separated on the operating table, the carcass was retained, the skin was manually peeled, and the fan-shaped bones were extracted. The *S. oualaniensis* carcasses were cut into small pieces, and 0.1 mol/L of citric acid solution was applied to clean the carcasses twice. The impurities were removed from the surface of the carcasses, and then they were weighed. The carcass was mixed with 0.1 mol/L NaOH at a sample-to-solution

ratio of 1:3 ($w/v$) to remove water-soluble substances, and the alkali solution was replaced 6 h later. The mixture was then centrifuged at 3000× $g$ for 10 min using a Himac CR 21G high-speed floor centrifuge (Hitachi, Tokyo, Japan), and 6 mol/L HCl was added to adjust the supernatant to pH 5.5. The precipitation was collected after centrifugation, and the prepared protein was freeze-dried in a vacuum and then stored in plastic bags in a freezer at −80 °C until further use.

### 2.3. Preparation of PHCSO, PHCSO-1 and PHCSO-2

In total, 1.0 g was weighed from the carcass protein of *S. oualaniensis* prepared in 2.2, with the addition of deionized water to adjust the substrate concentration to 4%. Then, pepsin with a substrate ratio of 9 U/mg was incubated at 37 °C for 4 h to initiate enzymolysis, and the resulting hydrolysate was named PHCSO. Half of the PHCSO was stored in plastic bags in a freezer at −80 °C until further use, and the other half was ultrafiltered at 4000× $g$ for 15 min with a test tube with a molecular weight of 10 kDa. The fraction with molecular weight > 10 kDa and <10 kDa were named PHCSO-1 and PHCSO-2, respectively.

### 2.4. Molecular Pattern

The molecular chromatogram of the protein isolated from the carcass of *S. oualaniensis* was determined by using sodium dodecyl sulfate–polyacrylamide gel electrophoresis (SDS-PAGE) according to Laemmli's method [17]. The samples were prepared with SDS to obtain 8 mg/mL. The samples were mixed with (3:1) 4 × Laemmli Sample Buffer (SDS, Tris-HCl, bromophenol blue, glycerol, and DTT) and oscillated slightly with a scroll oscillator (TianGen Biotech Co, Ltd., Beijing, China). The samples were boiled for 6 min, and the boiled mixture was briefly centrifuged at 2000× $g$. The test samples and standard protein marker (MW ranging from 35 kDa to 180 kDa) (Bio-Rad Laboratories Inc., Hercules, CA, USA) were loaded onto 5% stacking polyacrylamide gel with 8% separating gel (Cat# PG112, EpiZyme Biotechnology, Shanghai, China). The electrophoretic unit voltage is set to 80 V for the concentrated gel and 120 V for the separation gel. After the electrophoresis, the gel was stained with 0.25% Coomassie brilliant blue R-250 solution for 30 min and discolored with the mixture of 20% ($v/v$) ethanol and 10% ($v/v$) acetic acid twice, each for 1 h until clear protein bands were observed. The protein bands were then captured using the gel documentation system (Clinx GenoSens 2100(T), Shanghai, China).

### 2.5. Amino Acid Composition

The freeze-dried samples were completely hydrolyzed in 6 mol/L HCl at 110 °C for 24 h. The excess solvent was evaporated, and the drying process was repeated until the dried sample was dissolved in distilled water. The dried sample was finally dissolved with a minimum amount of sodium citrate buffer solution (pH 2.2) and filtered through a 0.45 nm hydrophilic membrane. The samples' amino acid content was analyzed using an amino acid analyzer (Hitachi LA-8080, Tokyo, Japan) [18].

### 2.6. Fourier Transform Infrared Spectroscopy (FTIR) Analysis

The 2 mg freeze-dried sample was mixed with dried KBr (100 mg) in order to make a 13 × 1 mm thin transparent disk by subjecting a pressure of approximately 5 × $10^6$ Pa and subjected to FTIR analysis using an FT/IR-400 spectrometer (PerkinElmer, Waltham, MA, USA) 4000–600 $cm^{-1}$ (mid-IR region) at 25 °C.

### 2.7. Determination of Antioxidant Activity

a. DPPH radical scavenging activity

PHCSO, PHCSO-1 and PHCSO-2 were diluted with deionized water into a 3 mg/L solution, respectively. A 2 mL sample was thoroughly mixed with 2 mL of 0.1 mmol/L DPPH, which was denoted as a sample group. A 2 mL sample was thoroughly mixed with 2 mL of ethanol and recorded as a blank group. A 2 mL measure of deionized water

was mixed with 2 mL of 0.1 mmol/L DPPH solution, which was recorded as the control group. Each group was reacted at room temperature for 40 min in the dark, and then the absorbances were measured at 517 nm with an ultraviolet spectrophotometer (UV-1800, Shimazu Earthquake Co., Kyoto, Japan). The free radical scavenging rate of sample DPPH was calculated as follows: DPPH radical scavenging activity (%) = [1 − (A1 − A2)/(A3 − A2)] × 100 where A1, A2 and A3 represent the absorbances of the sample, blank and control, respectively.

b. Hydroxyl radical scavenging activity

A 0.5 mL measure of $FeSO_4$ solution (9 mmol), 0.5 mL of salicylic acid–ethanol solution (9 mmol) and 5 mL of distilled water were mixed with 1 mL of sample in sequence. Then, the reaction was initiated by the addition of 0.5 mL of $H_2O_2$ (8.8 mmol) and incubated for 20 min at 37 °C. Distilled water instead of the sample was used as a control group, and distilled water instead of the $H_2O_2$ was used as a blank group. The absorbance at 510 nm was measured using an ultraviolet spectrophotometer. The hydroxyl scavenging activity of the sample was calculated as follows: hydroxyl radical scavenging activity (%) = [1 − (A1 − A2)/(A3 − A2)] × 100, where A1, A2 and A3 represent the absorbances of the sample, blank and control, respectively.

### *2.8. HSF Cells Culture*

HSF cells were removed from liquid nitrogen for resuscitation and maintained in DMEM (containing 10% FBS, 1.5% penicillin–streptomycin) under the conditions of 5% $CO_2$ and saturated humidity at 37 °C, digested with trypsin solution, and passaged every 48 h. Cells under good growth conditions and in the log phase were subjected to follow-up experiments.

### *2.9. Effect of PHCSO-1 and PHCSO-2 on Cell Viability of HSF Cells*

The CCK-8 kit was used to detect the effects of PHCSO and PHCSO-2 on the viability of the HSF cells. The HSF cells in the logarithmic growth stage were cultured in 96-well plates, and about $1 \times 10^4$ cells per well were cultured in a cell incubator for 24 h. Different concentrations (1, 2, 3, 4 and 5 mg/mL) of PHCSO and PHCSO-2 were added to the HSF cells, respectively, and DMEM was added as a blank group. Absorbance was measured at 450 nm using a microplate reader (SH-1000, Hitachi, Japan) after cell culture for 24 h.

### *2.10. Establishment of $H_2O_2$-Induced Oxidative Stress Model of HSF Cells*

The CCK-8 kit was used to detect the viability of HSF cells. HSF cells at the logarithmic growth stage were cultured in 96-well plates, and about $1 \times 10^4$ cells per well were cultured in a cell incubator for 24 h. Different concentrations (10, 20, 30, 50, 100, 500 and 1000 μmol/L) of $H_2O_2$ were added to HSF cells, and DMEM was added as a blank group. The absorbance was measured at 450 nm using a microplate reader (SH-1000, Hitachi, Japan) after cell culture for 1 h.

### *2.11. PHCSO and PHCSO-2 Repair HSF Cells from Oxidative Stress Induced by $H_2O_2$*

The CCK-8 kit was used to detect the viability of the HSF cells. The HSF cells in the logarithmic growth stage were cultured in 96-well plates, and about $1 \times 10^4$ cells per well were cultured in a cell incubator for 24 h. The HSF cells were pretreated with different concentrations (1, 2, 3, 4 and 5 mg/mL) of PHCSO and PHCSO-2, respectively, while only DMEM was added to the control group and the injured group. After 24 h, 20 μmol/L $H_2O_2$ was added to each well, and the cells were placed in the incubator for 1 h. Then, the absorbance was measured at 450 nm using a microplate reader (SH-1000, Hitachi, Japan).

### *2.12. ROS Fluorescence Staining*

The HSF cells in the logarithmic growth stage were cultured in 24-well plates, and about $1 \times 10^5$ cells per well were cultured in a cell incubator for 24 h. Different concentrations of PHCSO-2 (1, 2, 3, 4 and 5 mg/mL) were added to the HSF cells, while only DMEM

was added to the control group and injured group. After 24 h, 20 μmol/L $H_2O_2$ was added to each well, and the cells were placed in an incubator for 1 h and then washed twice with PBS buffer solution. At last, 10 μmol/L DCFH-DA was added to each well. After 30 min, the solution was removed and washed twice with PBS buffer solution and then observed under an inverted fluorescence microscope (BDS200-FL, Chongqing Optec Instrument Co., Ltd, Chongqing, China).

### *2.13. Effect of PHCSO-2 on Intracellular Antioxidant and Inflammatory Factors*

The HSF cells in the logarithmic growth stage were cultured in 6-well plates, and about $2 \times 10^5$ cells per well were cultured in a cell incubator for 24 h. Different concentrations of PHCSO-2 (1, 2, 3, 4 and 5 mg/mL) were added to the HSF cells, while only DMEM was added to the control group and injured group. After 24 h, 20 μmol/L $H_2O_2$ was added to each well, and the cells were placed in an incubator for 1 h. (a) The supernatant was collected after centrifugation of 2000× *g* for 30 min. The ELISA detection kit method was used to detect the contents of IL-1, IL-6 and TNF-α. (b) The cells were washed twice with PBS buffer, and 300 μL of RIPA lysis buffer was added. The adherent cells were lysed on ice for 20 min and centrifuged at 10,000× *g* for 5 min. The SOD activity and CAT activity and the GSH and MDA content in the adherents were detected in strict accordance with the kit instructions.

### *2.14. Statistical Analysis*

Each experiment was replicated three times. The data were expressed as mean ± standard deviation, and they are mentioned in the figure legends. Statistical analysis was performed using GraphPad Prism 9 software (GraphPad Inc., San Diego, CA, USA) using two-way ANOVA with Fisher's LSD test multiple comparison analysis. The values identified as outliers were excluded from the statistical analysis. The results were considered statistically significant if the $p$-value < 0.05.

## 3. Results

### *3.1. SDS-PAGE Protein Pattern*

The electrophoretic protein pattern of the carcass protein from *S. oualaniensis* is presented in Figure 1. The protein consists of seven bands with molecular weights of 240~200, 175, 60, 55, 44 and 36 kDa, respectively. The 240~200 kDa protein is MHC, the molecular weight of about 99 kDa protein indicates PM, the molecular weight of about 44 kDa indicates A, and the relatively small molecular weight indicates TM, which is about 36 kDa. Among them, the band of MHC is wide and thick, and this part of the proteins has a greater mass and content of similar molecules, and the protein band is clear, without the aggregation and degradation of macromolecular proteins caused by the acid–base treatment. The molecular size and amino acid composition of the protein isolates are closely related to their physicochemical and functional properties.

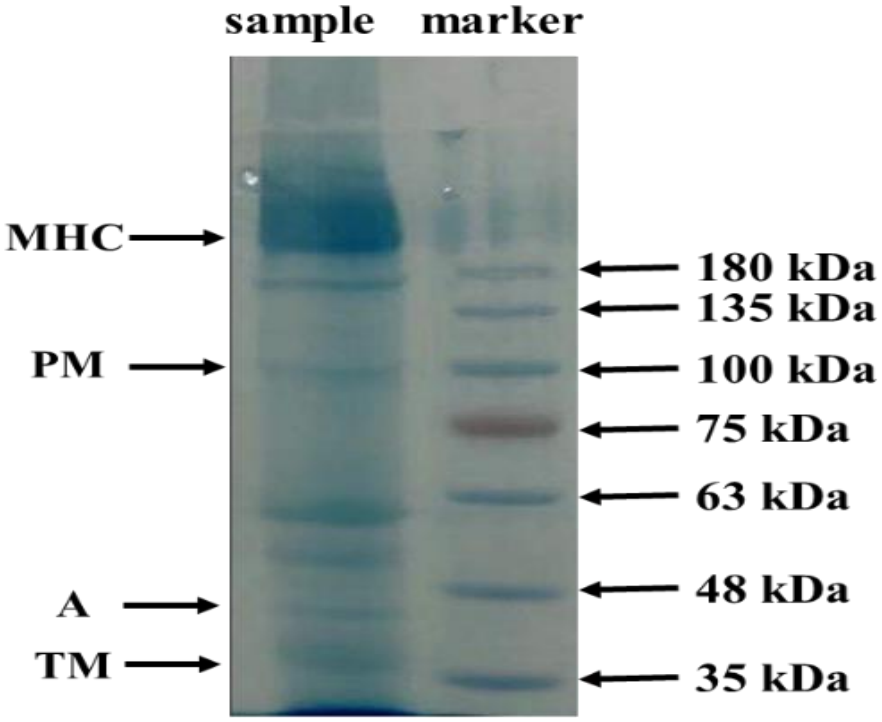


**Figure 1.** SDS-PAGE patterns of the carcass protein from *S. oualaniensis* and standard protein marker. MHC is myosin heavy chain; PM is paramyosin; A is actin; and TM is tromyosin.

### *3.2. Amino Acid Composition*

Automatic amino acid analysis was used to detect 17 amino acids from the carcass protein of *S. oualaniensis*, and the results are shown in Table 1.

**Table 1.** Amino acid composition and content of carcass protein from *S. oualaniensis*.

| | Amino Acid | Content (g/100 g) | Percentage of Total Amino Acids % |
|---|---|---|---|
| Polar amino acid | Glycine (Gly) | 2.46 | 4.12 |
| | Tyrosine (Tyr) | 2.43 | 4.06 |
| | Serine (Ser) | 2.73 | 4.58 |
| | Threonine (Thr) | 2.90 | 4.86 |
| Nonpolar amino acid | Alanine (Ala) | 3.43 | 5.74 |
| | Valine (Val) | 3.04 | 5.11 |
| | Leucine (Leu) | 5.59 | 9.38 |
| | Isoleucine (Ile) | 3.27 | 5.48 |
| | Phenylalanine (Phe) | 2.69 | 4.51 |
| | Proline (Pro) | 0.93 | 1.56 |
| | Tryptophan (Try) | 0.61 | 1.02 |
| | Methionine (Met) | 1.97 | 3.30 |
| Amino acids with negative charged | Lysine (Lys) | 5.31 | 8.91 |
| | Arginine (Arg) | 4.63 | 7.77 |
| | Histidine (His) | 1.77 | 2.97 |
| Amino acids with positive charge | Aspartic (Asp) | 6.34 | 10.63 |
| | Glutamic (Glu) | 9.54 | 16.00 |

The contents of the essential amino acids, Leu, Lys, Val and Ile, were higher in PHCSO, which were 5.59, 5.31, 3.04 and 3.27 g/100 g, respectively, accounting for 42.56% of the total amino acids. According to the ideal model of protein proposed by FAO/WHO, a protein is of good quality when its essential amino acids account for more than 40% of the total amino acids. The proportion of the essential amino acids and non-essential amino acids in

the carcass protein was suitable, and the nutrient structure was reasonable. Amino acids commonly contained in antioxidant peptides include Met, Arg, Leu, Ala and Glu, which account for 42.19% of the total amino acids in the carcass protein.

### 3.3. Fourier Transform Infrared (FTIR) Spectra

The FTIR transmission spectra of the carcass protein from *S. oualaniensis* are shown in Figure 2. Protein had general transmission patterns in major amide bands such as amide A, amide B, amide I, amide II and amide III, respectively. The maximum transmission wave numbers of amide A and amide B, which represent N-H stretching and $CH_2$ asymmetric stretching, respectively, were 3290 and 2934 $cm^{-1}$, respectively. Amide I of PHCSO was observed at 1643 $cm^{-1}$, which was mainly related to the C=O stretching vibration on the polypeptide backbone. The presence of amide II in PHCSO at 1539 $cm^{-1}$ is the result of the coupling of N-H bending vibration and CN tensile vibration. The absorption peak of amide III is located at 1235 $cm^{-1}$ and is related to intermolecular interactions, including N-C-N stretching and the N-H deformation of the amide bonds.

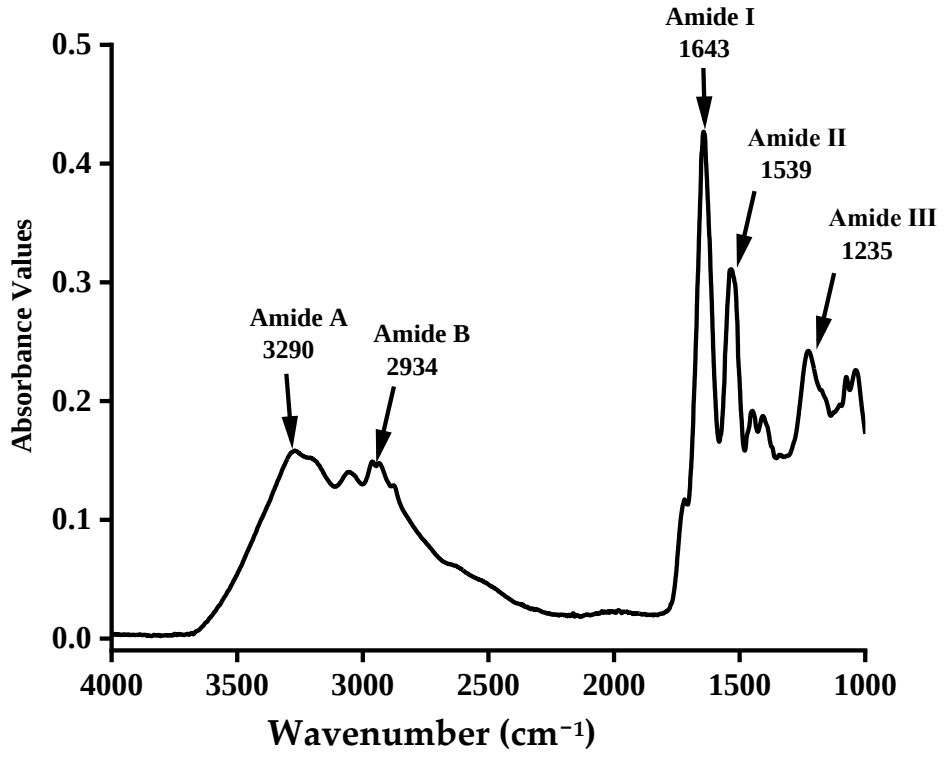


**Figure 2.** FTIR spectra of carcass protein from *S. oualaniensis*.

### 3.4. Analysis of Antioxidant Activity of PHCSO, PHCSO-1 and PHCSO-2

From the perspective of amino acid composition, the carcass protein from *S. oualaniensis* has the potential to prepare antioxidant peptides. The results of the DPPH radical scavenging activity and hydroxyl radical scavenging activity are shown in Figure 3. The results showed that the antioxidant activity of PHCSO-1 was weak, and small-molecule PHCSO-2 had higher DPPH and hydroxyl radical scavenging activity, but there was no significant difference when compared with PHCSO ($p < 0.05$). PHCSO-2 at a dosage of 5 mg/mL improves the DPPH radical scavenging activity and hydroxyl radical scavenging activity by 58% and 57%, respectively. Therefore, PHCSO and PHCSO-2 will be selected to explore the influence at the cellular level further.

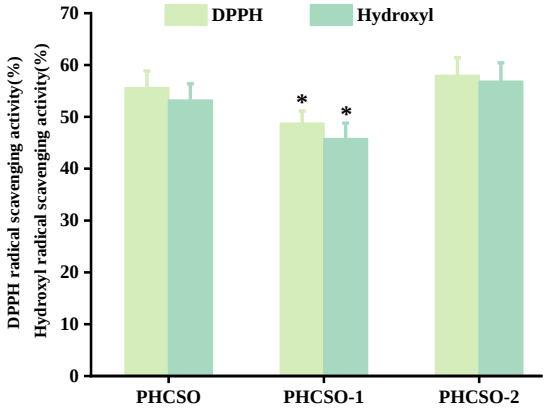


**Figure 3.** The antioxidant properties of PHCSO, PHCSO-1 and PHCSO-2. (* $p < 0.05$, vs. PHCSO).

### *3.5. The Effect of PHCSO and PHCSO-2 on the Viability of HSF Cells*

Cytotoxicity assay is a typical test used for drug safety. To ensure the effect of PHCSO and PHCSO-2 on HSF cells, the CCK-8 kit was used to determine the cell viability of the HSF cells with different concentrations of PHCSO and PHCSO-2. As can be seen from Figure 4A,B, PHCSO, and PHCSO-2 showed a dose-dependent proliferation effect on HSF cell viability, with significant differences compared with the blank group at 4 and 5 mg/mL ($p < 0.05$). At 5 mg/mL, the proliferation effect of PHCSO and PHCSO-2 on HSF cell viability was the highest, which were 126% and 133%, respectively. However, the overall proliferation rate of the HSF cells induced by PHCSO-2 was higher than that of PHCSO.

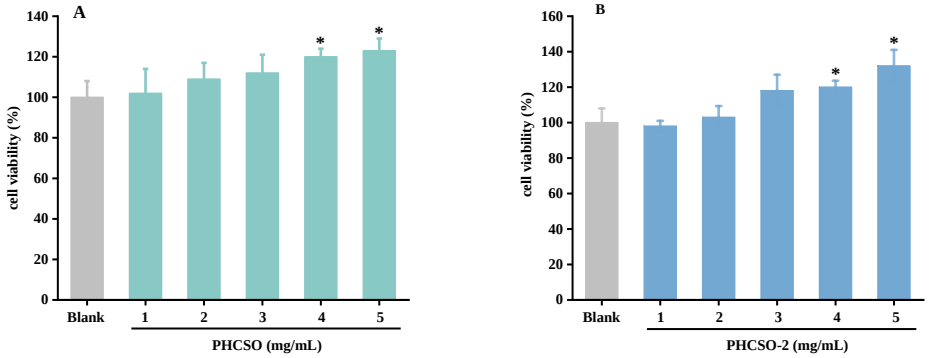


**Figure 4.** The effect of PHCSO (**A**) and PHCSO-2 (**B**) on the cell viability of HSF cells. Blank: blank control. (* $p < 0.05$, vs. the blank control).

### *3.6. Repair Effect of PHCSO and PHCSO-2 on $H_2O_2$-Induced Oxidative Stress of HSF Cells*

The effects of seven $H_2O_2$ concentration gradients (10, 20, 30, 50, 100, 500 and 1000 μmol/L) on the proliferation of HSF cells were studied to obtain the tolerance of HSF cells to $H_2O_2$ (Figure 5A). The results of CCK-8 cell proliferation showed that $H_2O_2$ inhibited HSF cell proliferation. Compared with the blank control group, the cell viability significantly decreased with the increase in $H_2O_2$ concentration ($p < 0.05$). The survival rate of the cells treated with 20 μmol/L $H_2O_2$ was 48%, which was close to half of the cell survival rate; therefore, the concentration was selected to establish the cell damage model. Cell survival was measured using a CCK-8 kit to evaluate the repair effect of PHCSO and PHCSO-2 on the $H_2O_2$-induced oxidative stress of HSF cells (Figure 5B,C). Both PHCSO and PHCSO-2 had certain repair effects on HSF cell damage induced by 20 μmol/L $H_2O_2$. The repair effect was dose-dependent and significantly different from the injured control group except for the addition of 1 mg/mL PHCSO ($p < 0.05$). When 5 mg/mL PHCSO-2 was added, the cell viability was as high as 96%. In addition, compared with PHCSO, PHCSO-2 has a higher repair effect on HSF cells, and when considering the production cost, PHCSO-2 was selected for the follow-up study on the antioxidant mechanisms.

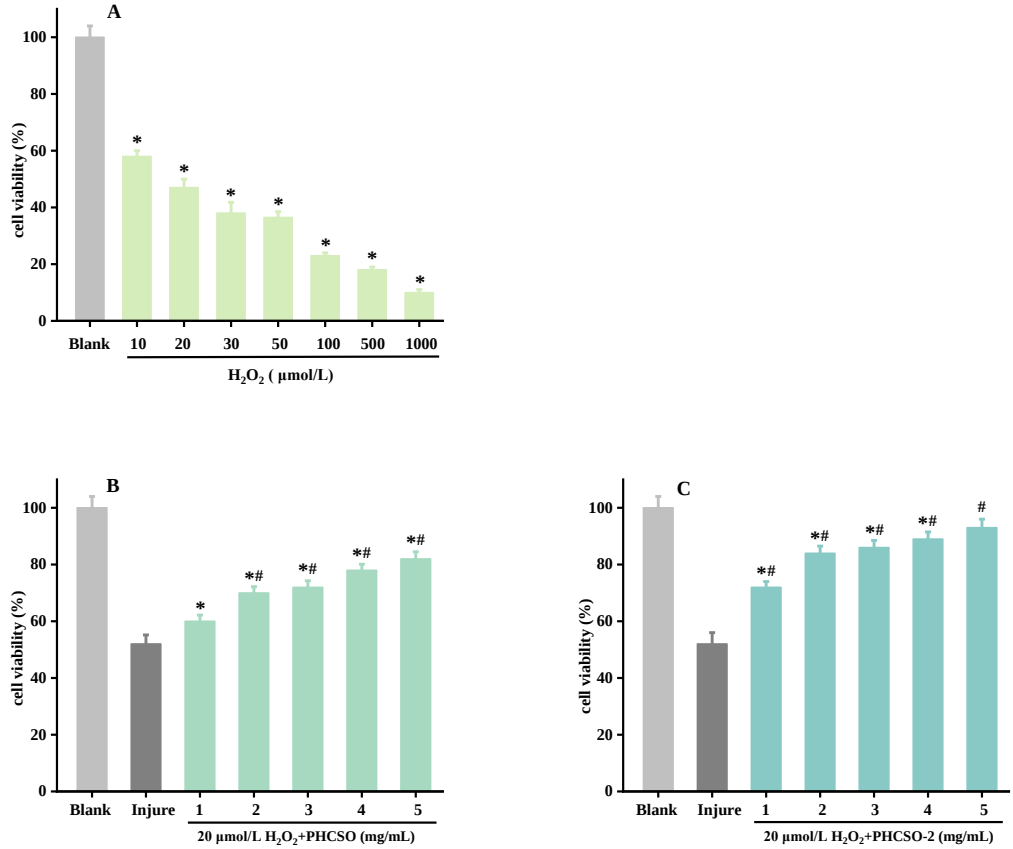


**Figure 5.** Effects of different concentrations of $H_2O_2$ on the cell viability of HSF cells (**A**). Effects of different concentrations of PHCSO-2 (**B**) and PHCSO (**C**) on the cell viability of oxidatively stressed HSF cells. Blank: blank control. Injured: injured control. (# $p < 0.05$ vs. the injured control, * $p < 0.05$, vs. the blank control).

### *3.7. Cell Morphology Observation and Repair Effects*

Figure 6A shows the effect of different concentrations of PHCSO-2 on the morphology of HSF cells. In the blank control, the number of cells was small and adherent, and the cell morphology was spindly and fibrous. The addition of PHCSO-2 increased cell density in a dose-dependent manner. The highest cell density was obtained when the added concentration reached 5 mg/mL. Figure 6B shows the effect of different concentrations of PHCSO-2 on the morphology of HSF cells under oxidative stress. The cells in the injured control group were small and loosely arranged and mostly composed of floating dead cells. However, with the increase in PHCSO-2 concentration, the number of adherent cells increased in a dose-dependent manner. When 5 mg/mL PHCSO-2 was added, the cell density was the highest, and the fibroblast morphology was obvious. Intracellular ROS production was evaluated using DCFH-DA to reflect the repair effect of PHCSO-2 on cells pretreated with $H_2O_2$, as shown in Figure 6C. ROS production was significantly increased in cells exposed to $H_2O_2$, and cells in the injured control group were small, loosely arranged, and had strong fluorescence intensity. When the concentration was 5 mg/mL, the fluorescence intensity decreased, indicating that 5 mg/mL PHCSO-2 could effectively reduce the production of ROS.

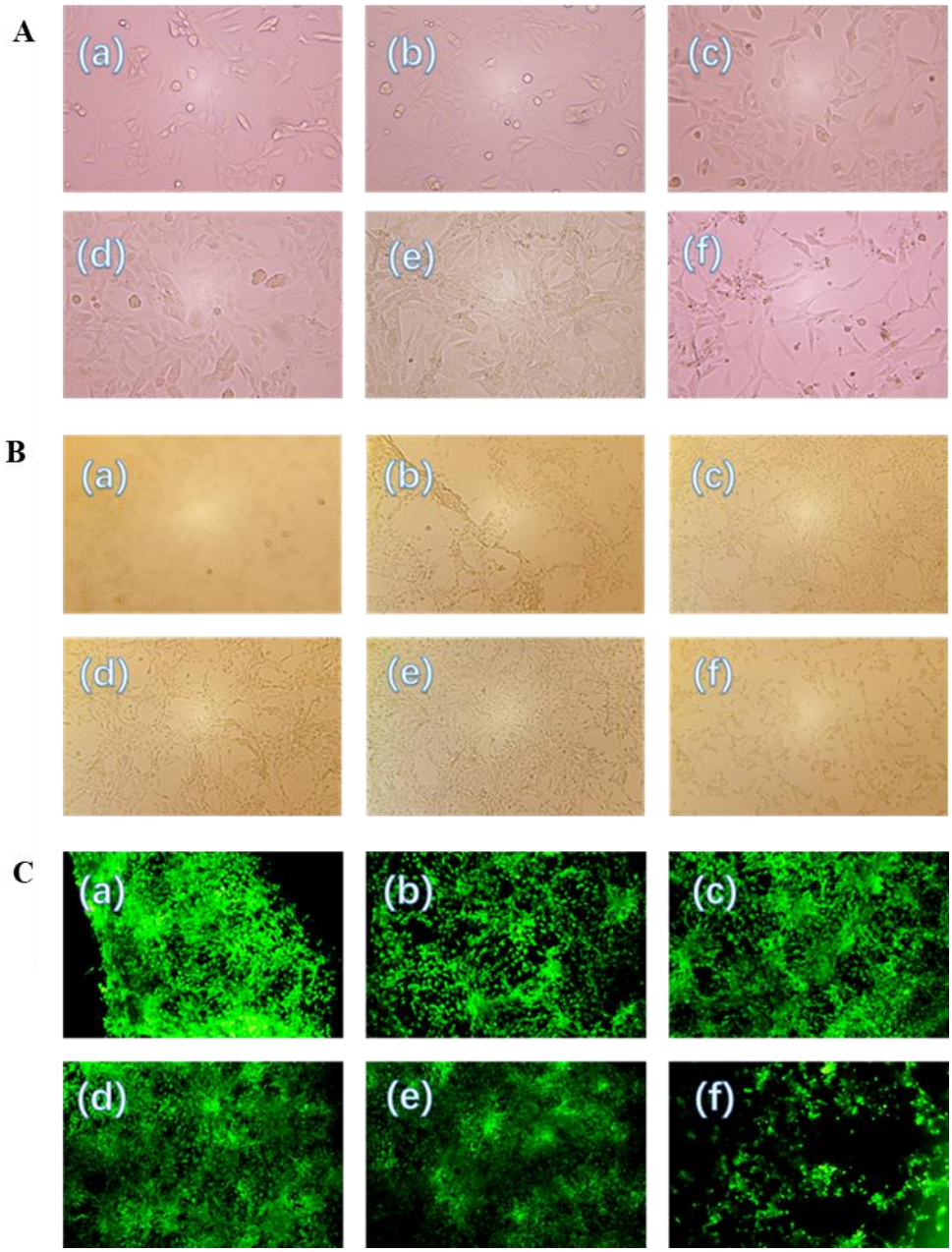


**Figure 6.** Morphological observation diagram of the effect of different concentrations of PHCSO-2 on HSF cells (**A**). (a–e) add 1, 2, 3, 4 and 5 mg/mL PHCS-2, respectively, and (f) is blank control. Morphological observation diagram (**B**) and fluorescence staining observation diagram (**C**) of the effect of different concentrations of PHCSO-2 on HSF cells under oxidative stress. In total, 20 μmol/L $H_2O_2$ was added to (a–f), and 1, 2, 3, 4 and 5 mg/mL PHCS-2 were added to (a–e), respectively. (f) is the injured control.

### *3.8. Intracellular SOD, CAT, GSH and MDA Level*

The activity of antioxidant enzymes has a great influence on cell growth and senescence. SOD, CAT, GSH and MDA are necessary indexes to detect the level of intracellular free radicals. Compared with blank control, SOD (Figure 7A), CAT (Figure 7B) and GSH (Figure 7C) contents in the injured control were significantly decreased, while MDA (Figure 7D) contents were significantly increased, indicating that the antioxidant capacity of cells after $H_2O_2$ oxidation was significantly decreased. Compared with the injured control, SOD, CAT and GSH contents increased, and MDA contents decreased after the addition of PHCSO-2, indicating that PHCSO-2 had a good repair effect on HSF cells damaged

by $H_2O_2$ oxidation. When the concentration of PHCSO-2 increased in the range of 1–5 mg/mL, the antioxidant capacity of cells gradually increased. Therefore, PHCSO-2 may act as an antioxidant in a similar manner to GSH to prevent $H_2O_2$-induced oxidative stress in HSF cells.

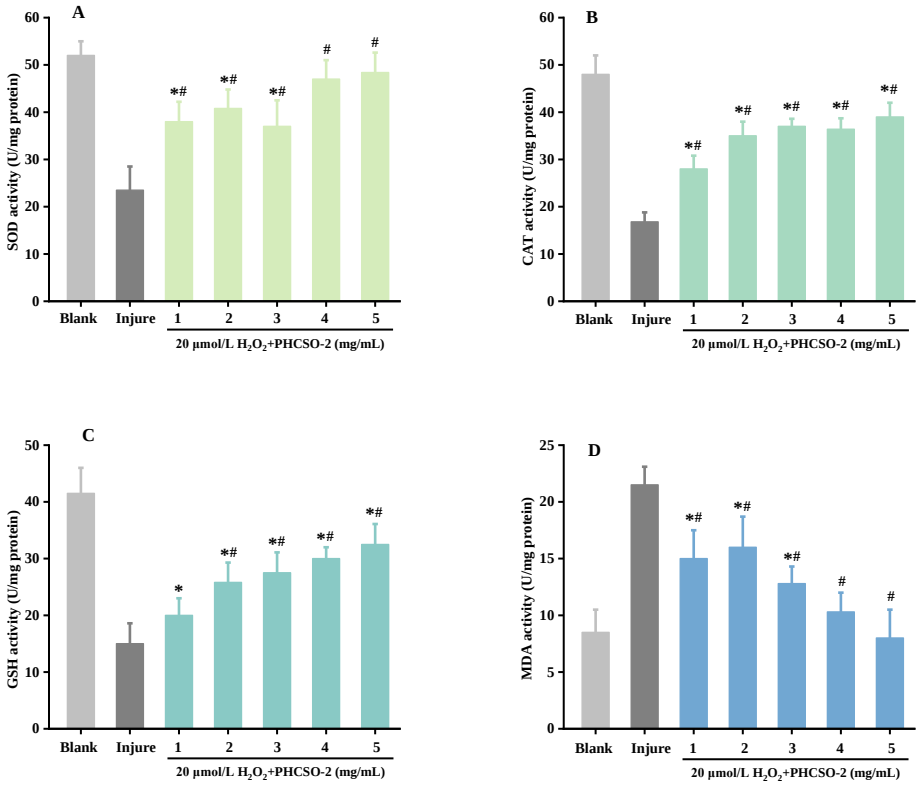


**Figure 7.** The effect of different concentrations of PHCSO-2 on the activity of SOD (**A**), CAT (**B**), GSH (**C**) and MDA (**D**) in HSF under $H_2O_2$ oxidative stress. Blank: blank control. Injure: injured control. (# $p < 0.05$ vs. the injured control, * $p < 0.05$, vs. the blank control).

### *3.9. The Inflammatory Factors IL-1, IL-6 and TNF-α Level*

The contents of IL-1 (Figure 8A), IL-6 (Figure 8B) and TNF-α (Figure 8C) induced by oxidative stress were determined using ELISA to observe the occurrence of inflammation. As shown in Figure 8, compared with the blank control, the contents of IL-1, IL-6 and TNF-α in the injured control were significantly increased, indicating that $H_2O_2$-induced oxidative stress induced a significant increase in the levels of inflammatory factors and inflammation in HSF cells. After the addition of PHCSO-2, inflammatory expression levels were reduced in a dose-dependent manner in the range of 1 to 5 mg/mL. When 5 mg/mL PHCSO-2 was added, the contents of IL-1, IL-6 and TNF-α were significantly decreased ($p < 0.05$); however, the difference was not statistically significant compared with the blank control. Therefore, PHCSO-2 has a good inhibitory effect on the inflammatory factors produced through the oxidative stress of $H_2O_2$.

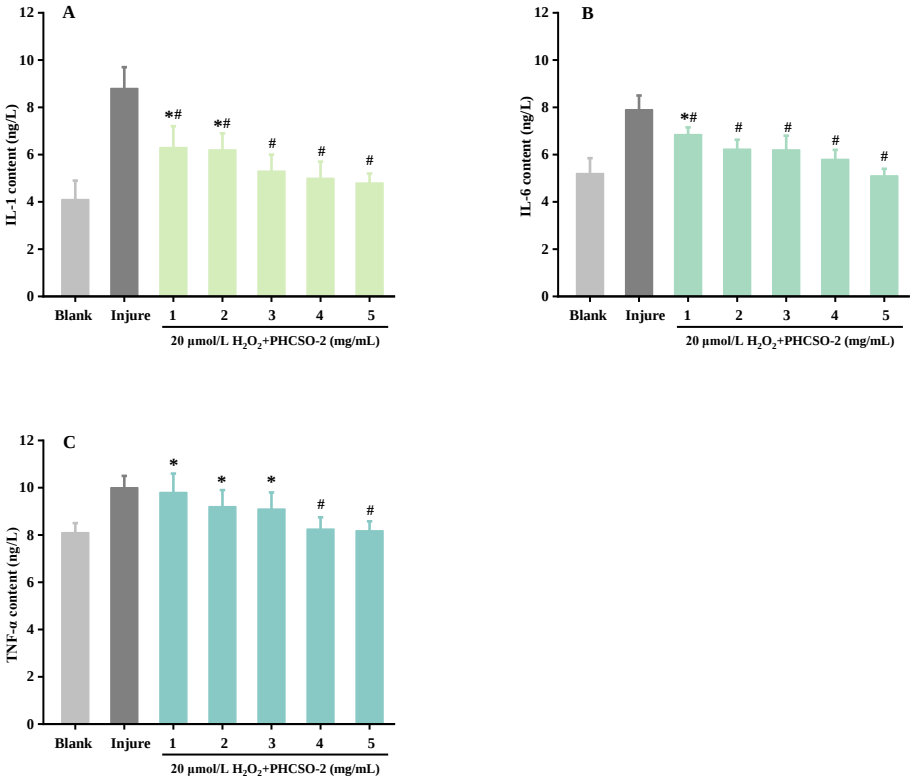


**Figure 8.** The effect of different concentrations of PHCSO-2 on the content of IL-1 (**A**), IL-6 (**B**) and TNF-α (**C**) in HSF under $H_2O_2$ oxidative stress. Blank: blank control. Injure: injured control. (# $p < 0.05$ vs. the injured control, * $p < 0.05$, vs. the blank control).

## 4. Discussion

According to the SDS-PAGE protein profile, the carcass protein from *S. oualaniensis*, through the use of an alkali solution and acid isolation, showed clear bands with no obvious aggregation or degradation, which indicated the compatibility of pepsin in the extraction of the carcass protein. The carcass protein contains over 40% essential amino acids, including high contents of leucine and lysine. Similar to salmon, *S. oualaniensis* produced a high-quality aquatic protein with reasonable composition, which conforms to the ideal structural pattern of a high-quality protein proposed by the WHO [12,19]. Antioxidant amino acids, such as Met, Arg, Leu, Ala and Glu, compose about 42.19% of the peptides from carcass protein, indicating its potential to produce antioxidant peptides. Given the fact that peptides of low molecular weight commonly have high antioxidant activity, PHCSO-2 has reasonably better DPPH and hydroxyl radical scavenging activity than PHCSO-1, which is also supported by the study on cottonseed protein hydrolysates (<3 kDa) [20].

In this study, both PHCSO and PHCSO-2 improved the viability of HSF cells without cytotoxicity, between which PHCSO-2 possessed better protection than PHCSO. Since the theory of replicative aging was proposed, $H_2O_2$, UV and many other methods have been applied to construct cell damage models [21], among which $H_2O_2$ is usually used to induce oxidative stress on cells for antioxidant screening in vitro [22]. DNA damage is caused by oxidative stress via the activation of the P53/P21 signaling pathway, whose expressions are closely related to the cell cycle and apoptosis. The increasing level of the P21 gene inhibits the activity of CDK4/6, followed by the blocking of the cell cycle, which consequently results in cell growth arrest and cell senescence delay [23,24]. Therefore, PHCSO-2 was selected for further investigations, including cell observation, fluorescence staining, antioxidant enzyme activity and inflammatory factor assay.

DCFH-DA was used to evaluate intracellular ROS production by producing 2′, 7′-dichlorofluorescein (DCF) after the hydrolyzation and oxidation in cells that can emit

green fluorescence under the stimulation of $H_2O_2$ [25]. Although reactive oxygen species (ROS) are a natural byproduct of normal oxygen metabolism in mitochondria, an excessive amount of them is harmful to cell function and homeostasis [26]. By degrading extracellular matrix proteins (such as collagen) and changing connective tissue, ROS could accelerate skin aging [27]. ROS can also directly damage DNA, lipids and proteins in dermal cells [28] and alter transcription. In contrast, more than half of the HSF cells were apoptotic in the injured group, and the 5 mg/mL PHCSO-2 pretreated group showed vigorous growth of cells, with decreasing intracellular ROS levels.

SOD, CAT, GSH and MDA are important indicators for the detection of the level of free radicals in cells. SOD and CAT are both important antioxidant enzymes for scavenging free radicals in cells [29,30]. In general, endogenous antioxidant enzymes can effectively protect against skin damage through ROS clearance [31]. Reduced GSH is a tripeptide that helps maintain the normal immune function of the human body with detoxification and antioxidative effects [32]. MDA is one of the key substances of lipid peroxidation in cells [33]. To assess the antioxidant effect of PHCSO-2, key oxidation resistance genes, including SOD, CAT, and GSH, and the oxidation product MDA, were investigated for their expression. According to the results, SOD, CAT and GSH transcripts in PHCSO-2 pretreated HSF cells were significantly up-regulated, while MDA transcripts were significantly down-regulated, compared to the injured group. In addition, it can also reduce the susceptibility of cells to secondary oxidative stress.

The secretion of pro-inflammatory cytokines and the release of pro-inflammatory mediators induced by oxidative stress led to the infiltration of inflammatory cells into the dermis, resulting in skin damage, accelerating skin aging and even skin cancer [34]. Therefore, inflammatory cytokines are the most intuitive factors for the estimation of inflammation. As proven in a previous study, low-molecular peptides extracted from salmon and chicken inhibit the expressions of nuclear factor κ-B (NF-kB) and inducible nitric oxide synthase (iNOS), respectively [35,36]. Using a pretreatment of 5 mg/mL PHCSO-2, IL-1 almost keeps a similar transcription level with that of the blank group in HSF cells. Compared to the injured HSF cells, both the IL-6 and TNF-α transcripts were significantly down-regulated in PHCSO-2 pretreated cells under oxidative stress induced through the use of $H_2O_2$, which indicates the protective effect on the skin against oxidative stress.

## 5. Conclusions

In the present study, PHCSO-1 and PHCSO-2, with molecular weights of <10 kDa and >10 kDa, were isolated from the PHCSO of *S. oualaniensis* through ultrafiltration followed by an investigation of their antioxidant activities. Among the peptides, PHCSO-2 had better antioxidant properties. Similarly, PHCSO-2 showed low cytotoxic and higher protective effects than PHCSO, as evidenced by the $H_2O_2$-induced HSF cell damage model. In conclusion, the experiments concerning cell morphology, fluorescence staining, antioxidant enzyme activity and inflammatory factor evidenced that PHCSO-2 showed a significant antioxidant capacity in terms of the oxidation and inflammation caused by $H_2O_2$ injury on HSF cells. Therefore, PHCSO-2 could be used as a potential agent in cosmetics to effectively repair skin damage and anti-aging applications.

**Author Contributions:** W.W. and J.E., conceptualization, funding acquisition; N.L., formal analysis, investigation, writing—original draft preparation; X.D., X.P. and J.E., writing—review and editing; P.T., methodology. All authors have read and agreed to the published version of the manuscript.

**Funding:** Project supported by the National Natural Science Foundation of China (Grant No. 82173731). Project supported by the Research Fund for International Young Scientists (Grant No. 81750110548). Project supported by the Natural Science Foundation of Shanghai (No. 21ZR1427300).

**Institutional Review Board Statement:** Not applicable.

**Informed Consent Statement:** Not applicable.

**Data Availability Statement:** Not applicable.

**Conflicts of Interest:** The authors declare no conflict of interest.

## References


1. Vladkova, T.; Georgieva, N.; Staneva, A.; Gospodinova, D. Recent Progress in Antioxidant Active Substances from Marine Biota. *Antioxidants* **2022**, *11*, 439. [CrossRef]
2. Jakubczyk, K.; Dec, K.; Kałduńska, J.; Kawczuga, D.; Kochman, J.; Janda, K. Reactive oxygen species—Sources, functions, oxidative damage. *Pol. Merkur. Lekarski.* **2020**, *48*, 124–127. [PubMed]
3. Fisher, G.J.; Quan, T.; Purohit, T.; Shao, Y.; Cho, M.K.; He, T.; Varani, J.; Kang, S.; Voorhees, J.J. Collagen Fragmentation Promotes Oxidative Stress and Elevates Matrix Metalloproteinase-1 in Fibroblasts in Aged Human Skin. *Am. J. Pathol.* **2009**, *174*, 101–114. [CrossRef] [PubMed]
4. Valachová, K.; Topoľská, D.; Mendichi, R.; Collins, M.N.; Sasinková, V.; Šoltés, L. Hydrogen peroxide generation by the Weissberger biogenic oxidative system during hyaluronan degradation. *Carbohydr. Polym.* **2016**, *148*, 189–193. [CrossRef]
5. Peng, L.; Kong, X.; Wang, Z.; Ai-Lati, A.; Ji, Z.; Mao, J. Baijiu vinasse as a new source of bioactive peptides with antioxidant and anti-inflammatory activity. *Food Chem.* **2021**, *339*, 128159. [CrossRef]
6. Marcuse, R. Antioxidative Effect of Amino-Acids. *Nature* **1960**, *186*, 886–887. [CrossRef]
7. López-García, G.; Dublan-García, O.; Arizmendi-Cotero, D.; Gomez-Olivan, L.M. Antioxidant and Antimicrobial Peptides Derived from Food Proteins. *Molecules* **2022**, *27*, 1343. [CrossRef]
8. Sudhakar, S.; Nazeer, R.A. Structural characterization of an Indian squid antioxidant peptide and its protective effect against cellular reactive oxygen species. *J. Funct. Foods* **2015**, *14*, 502–512. [CrossRef]
9. Singh, A.; Hong, H.; Benjakul, S. Threadfin bream surimi gel containing squid fin protein hydrolysate: Textural properties, acceptability, and volatile profile. *J. Food Sci.* **2022**, *87*, 2337–2349. [CrossRef] [PubMed]
10. Zhang, Y.; Dai, B.; Deng, Y.; Zhao, Y. In vitro anti-inflammatory and antioxidant activities and protein quality of high hydrostatic pressure treated squids (*Todarodes pacificus*). *Food Chem.* **2016**, *203*, 258–266. [CrossRef]
11. Kerasioti, E.; Stagos, D.; Priftis, A.; Aivazidis, S.; Tsatsakis, A.M.; Hayes, A.W.; Kouretas, D. Antioxidant effects of whey protein on muscle C2C12 cells. *Food Chem.* **2014**, *155*, 271–278. [CrossRef]
12. Blanco-Pascual, N.; Fernández-Martín, F.; Montero, P. Jumbo squid (*Dosidicus gigas*) myofibrillar protein concentrate for edible packaging films and storage stability. *LWT-Food Sci. Technol.* **2014**, *55*, 543–550. [CrossRef]
13. Clemente, A. Enzymatic protein hydrolysates in human nutrition. *Trends Food Sci. Technol.* **2000**, *11*, 254–262. [CrossRef]
14. Dai, H.J.; Sun, Y.L.; Zheng, X.L.; Feng, Z.X.; Wen, J.; Zhao, J.; Chen, D.H. Extraction optimization, preliminary characterization and antioxidant activity of glycoproteins from the muscle of Sepia pharaonis. *Food Sci. Technol. Res.* **2016**, *22*, 39–52. [CrossRef]
15. Zhang, K.; Wei, R.; Song, R. Extraction of Cathepsin D-Like Protease from Neon Flying Squid (*Ommastrephes bartramii*) Viscera and Application in Antioxidant Hydrolysate Production. *Biomolecules* **2019**, *9*, 228. [CrossRef] [PubMed]
16. Liu, Q.; Yao, Y.; Ibrahim, M.A.A.; Halawany, A.M.E.; Yang, L.; Zhang, X. Production of Dual Inhibitory Hydrolysate by Enzymatic Hy-drolysis of Squid Processing By-product. *Mar. Biotechnol. (NY)* **2022**, *24*, 293–302. [CrossRef] [PubMed]
17. Laemmli, U.K. Cleavage of Structural Proteins during the Assembly of the Head of Bacteriophage T4. *Nature* **1970**, *227*, 680–685. [CrossRef]
18. Kittiphattanabawon, P.; Benjakul, S.; Visessanguan, W.; Shahidi, F. Isolation and characterization of collagen from the cartilages of brownbanded bamboo shark (*Chiloscyllium punctatum*) and blacktip shark (*Carcharhinus limbatus*). *LWT—Food Sci. Technol.* **2010**, *43*, 792–800. [CrossRef]
19. Food, J.; Organisation, A. World Health Organisation Ad Hoc Expert Committee. Energy and protein requirements. *FAO Nutr. Meet. Rep. Ser.* **1973**, *7*, 105–106.
20. Wang, L.; Ma, M.; Yu, Z.; Du, S.-K. Preparation and identification of antioxidant peptides from cottonseed proteins. *Food Chem.* **2021**, *352*, 129399. [CrossRef]
21. Park, M.J.; Bae, Y.S. Fermented *Acanthopanax koreanum* root extract reduces UVB-and $H_2O_2$-induced senescence in human skin fibroblast cells. *J. Microbiol. Biotechnol.* **2016**, *26*, 1224–1233. [CrossRef]
22. Feng, B.; Ma, L.J.; Yao, J.J.; Fang, Y.; Mei, Y.A.; Wei, S.M. Protective effect of oat bran extracts on human dermal fibroblast injury induced by hydrogen peroxide. *J. Zhejiang Univ. Sci. B* **2013**, *14*, 97. [CrossRef]
23. Zdanov, S.; Debacq-Chainiaux, F.; Remacle, J.; Toussaint, O. Identification of p38MAPK-dependent genes with changed transcript abundance in H2O2-induced premature senescence of IMR-90 hTERT human fibroblasts. *FEBS Lett.* **2006**, *580*, 6455–6463. [CrossRef]
24. Makpol, S.; Jam, F.A.; Khor, S.C.; Ismail, Z.; Mohd Yusof, Y.A.; Ngah, W.Z. Comparative effects of biodynes, tocotrienol-rich fraction, and tocopherol in enhancing collagen synthesis and inhibiting collagen degradation in stress-induced premature senescence model of human diploid fibroblasts. *Oxid. Med. Cell Longev.* **2013**, *2013*, 298574. [CrossRef]
25. LeBel, C.P.; Ischiropoulos, H.; Bondy, S.C. Evaluation of the probe 2′,7′-dichlorofluorescin as an indicator of reactive oxygen species formation and oxidative stress. *Chem. Res. Toxicol.* **1992**, *5*, 227–231. [CrossRef] [PubMed]
26. Nishigori, C.; Hattori, Y.; Toyokuni, S. Role of Reactive Oxygen Species in Skin Carcinogenesis. *Antioxidants Redox Signal.* **2004**, *6*, 561–570. [CrossRef] [PubMed]
27. Masaki, H.; Izutsu, Y.; Yahagi, S.; Okano, Y. Reactive Oxygen Species in HaCaT Keratinocytes After UVB Irradiation Are Triggered by Intracellular $Ca^{2+}$ Levels. *J. Investig. Dermatol. Symp. Proc.* **2009**, *14*, 50–52. [CrossRef]

28. Calabrese, V.; Calafato, S.; Puleo, E.; Cornelius, C.; Sapienza, M.; Morganti, P.; Mancuso, C. Redox regulation of cellular stress response by ferulic acid ethyl ester in human dermal fibroblasts: Role of vitagenes. *Clin. Dermatol.* **2008**, *26*, 358–363. [CrossRef]
29. Yang, J.; Xiong, Q.; Zhang, J.; Yan, S.; Zhu, L.; Zhu, B. The Protective Effect of *Stauntonia Chinensis* Polysaccharide on CCl4-induced Acute Liver Injuries in Mice. *Int. J. Biomed. Sci.* **2014**, *10*, 16–20. [PubMed]
30. Krych-Madej, J.; Gebicka, L. Do pH and flavonoids influence hypochlorous acid-induced catalase inhibition and heme modification? *Int. J. Biol. Macromol.* **2015**, *80*, 162–169. [CrossRef]
31. Xiong, Q.; Xie, P.; Li, H.; Hao, L.; Li, G.; Qiu, T.; Liu, Y. Acute effects of microcystins exposure on the transcription of antioxidant enzyme genes in three organs (liver, kidney, and testis) of male Wistar rats. *J. Biochem. Mol. Toxicol.* **2010**, *24*, 361–367. [CrossRef]
32. Hanko, M.; Švorc, Ľ.; Planková, A.; Mikuš, P. Overview and recent advances in electrochemical sensing of glutathione–A review. *Anal. Chim. Acta* **2019**, *1062*, 1–27. [CrossRef] [PubMed]
33. Yapislar, H.; Taskin, E. L-carnosine alters some hemorheologic and lipid peroxidation parameters in nephrectomized rats. *Med. Sci. Monit. Int. Med. J. Exp. Clin. Res.* **2014**, *20*, 399.
34. Kiyoshima, T.; Enoki, N.; Kobayashi, I.; Sakai, T.; Nagata, K.; Wada, H.; Fujiwara, H.; Ookuma, Y.; Sakai, H. Oxidative stress caused by a low concentration of hydrogen peroxide induces senescence-like changes in mouse gingival fibroblasts. *Int. J. Mol. Med.* **2012**, *30*, 1007–1012. [CrossRef] [PubMed]
35. Chevrier, G.; Mitchell, P.L.; Rioux, L.E.; Hasan, F.; Jin, T.; Roblet, C.R.; Doyen, A.; Pilon, G.; St-Pierre, P.; Lavigne, C.; et al. Low-Molecular-Weight Peptides from Salmon Protein Prevent Obesity-Linked Glucose Intolerance, Inflammation, and Dyslipidemia in LDLR-/-/ApoB100/100 Mice. *J. Nutr.* **2015**, *145*, 1415–1422. [CrossRef]
36. Sun, X.; Chakrabarti, S.; Fang, J.; Yin, Y.; Wu, J. Low-molecular-weight fractions of Alcalase hydrolyzed egg ovomucin extract exert anti-inflammatory activity in human dermal fibroblasts through the inhibition of tumor necrosis factor–mediated nuclear factor κB pathway. *Nutr. Res.* **2016**, *36*, 648–657. [CrossRef]